NASA Contractor Report 178235

ICASE REPORT NO. 87-6

ICASE

ERROR ESTIMATES FOR CELL-VERTEX SOLUTIONS

OF THE COMPRESSIBLE EULER EQUATIONS

P. L. Roe

Contract No. NAS1-18107

January 1987

INSTITUTE FOR COMPUTER APPLICATIONS IN SCIENCE AND ENGINEERING
NASA Langley Research Center, Hampton, Virginia 23665

Operated by the Universities Space Research Association

National Aeronautics and
Space Administration

Langley Research Center
Hampton, Virginia 23665-5225

ERROR ESTIMATES FOR CELL-VERTEX SOLUTIONS OF THE COMPRESSIBLE EULER EQUATIONS

P. L. Roe
Cranfield Institute of Technology, United Kingdom

ABSTRACT

The cell-vertex schemes due to Ni and Jameson, et al., have been subjected to a theoretical analysis of their truncation error. The analysis confirms the authors' claims for second-order accuracy on smooth grids, but shows that the same accuracy cannot be obtained on arbitrary grids. It is shown that the schemes have a unique generalization to axisymmetric flow that preserves the second-order accuracy.

This research was supported under the National Aeronautics and Space Administration under NASA Contract No. NAS1-18107 while the author was in residence at the Institute for Computer Applications in Science and Engineering (ICASE), NASA Langley Research Center, Hampton, VA 23665-5225.

1. Introduction

Most Euler codes written for computing inviscid aerodynamic flows have made use of the finite-volume formulation. An early example was described by Rizzi and Inouye [1]. Essentially, they are generalizations of the second-order accurate Lax-Wendroff [2] algorithm to nonrectangular mesh geometries. Conservation (which is a necessary ingredient toward ensuring convergence to correct weak solutions [3]) comes from regarding the numerical representation of the flow as comprising average states within each computational cell. The rules for updating these values employ interface fluxes which transfer the mass, momentum, and energy between neighboring cells, leaving the total quantities present unchanged except for boundary effects. There seems to be little analysis to indicate how accurate these schemes are on nonuniform grids. They are clearly second-order accurate on uniform, rectangular grids, and it has been generally assumed that second-order accuracy will still be obtained on a "sufficiently smooth" irregular grid.

Finite-volume schemes based on central-differencing algorithms have become very popular following the work of Jameson et al. [4]. Because these schemes update the solution via a five-cell rather than nine-cell stencil, their accuracy is easier to analyze and has been treated theoretically by Turkel [5], whose results have led to modified schemes offering better accuracy. Numerical experiments confirming this are reported by Turkel et al. [6].

Yet another possibility is the scheme recently introduced by Ni [7]. Here the numerical values represent states found at the corners (vertices) of the computational cells. Ni originally described his scheme in finite-difference terms, with the values approximating point samples of the continuum

solution. Subsequently, it has been described in finite-element terms with the vertex values implying a bilinear interpolation function within each cell (Davis et al. [8], Lohner et al. [9]). This latter view enables a precise interpretation of conservation to be given. At a time when various schools of thought are learning to use each other's language and ideas, we prefer to classify Ni's method under the neutral term of "cell vertex" scheme. One attraction of Ni's scheme (which has been very significantly refined by Hall [10]) is that it seems to handle arbitrary, even completely unsmooth, meshes in a very natural way. However, we will show that claims of uniformly second-order accuracy are based on an incorrect argument. The object of this paper is to provide a correct analysis of the accuracy of cell-vertex schemes.

This is made easier by the fact that these schemes, in a sense, factorize the process of updating the solution. Each cell is examined to see if the fluxes around it are in balance; if not, some changes are made. The updating process at each vertex uses nine vertex states so that, overall, the scheme is as complex as Lax-Wendroff. However, the test for balance involves only four vertices, making the first stage very amenable to analysis. This first stage is the only part to be analyzed here, but this is the only analysis needed to determine the accuracy of the steady state which is reached when all cells are in equilibrium. That is to say, the integral

$$\oint (\underline{F}\, dy - \underline{G}\, dx) \tag{1.1}$$

evaluated by the trapezium rule, vanishes around every cell (Figure 1a). Note that there are generally more vertices than cells so that this condition leaves the solution undetermined. Boundary conditions need to be added, but

carefully. If too many are prescribed, then the integral cannot vanish everywhere. Paisley [11] discusses these isues, including the role of boundary conditions in suppressing unwanted "checkerboard" modes in the solution. See also Morton and Paisley [12].

For problems that are geometrically complicated, or algorithms which employ local mesh refinement in difficult areas, it is attractive to use meshes composed of triangles, perhaps without any regular structure. Jameson et al. [13] have proposed a scheme which also makes use of flow variables located at vertices. Again, it is unclear whether to regard the values as point samples or as defining a finite-element interpolant (this time linear). Clearly, it is not now possible to require that the flux integral vanishes around the perimeter of every cell because, in a triangular mesh, vertices outnumber cells by roughly 2:1; so the problem would be overconstrained even without boundary conditions. Instead, Jameson's procedure is such that the solution ceases to change when the flux integral vanishes around all control volumes such as the one shown in Figure 1b.

The analysis contained in this paper applies equally to Ni's and to Jameson's schemes because it evaluates the accuracy of the approximate flux integral in terms of the geometry of the polygon around which it is evaluated. The claim, mentioned earlier, of second-order accuracy arising from the trapezium rule is fallacious because, as we refine the grid, the contour around which we integrate does not remain fixed but shrinks with the grid and always contains just a few intervals. In fact, it is easy enough to make an analysis based on a local two-dimensional Taylor expansion which demonstrates that the integrals are only evaluated to second-order accuracy if the polygons meet certain geometric criteria. These criteria are not met by any

triangle or by any quadrilateral except parallelograms. They are satisfied by all regular n-gons ($n > 3$) and in a seemingly sporadic manner by various irregular n-gons ($n > 4$). In practice, the errors will be acceptable if the polygons have sufficiently small error constants, the formulae for which are given.

There are two offshoots to our analysis. One is that we derive a consistent finite-element interpretation of the cell-vertex schemes. We show that it gives results which differ from those of the finite-difference interpretation by terms of the same magnitude as the truncation error inherent in either. Finally, we consider the application of these schemes to problems which are pseudo-two-dimensional, for example, axially symmetric. We show that out of a family of plausible extensions, only one member is capable of retaining second-order accuracy near the axis.

2. Description of Cell-Vertex Schemes

We consider steady inviscid two-dimensional compressible flow governed by the Euler equations

$$\frac{\partial \underline{F}}{\partial x} + \frac{\partial \underline{G}}{\partial y} = 0 \tag{2.1}$$

where

$$\underline{F} = \begin{pmatrix} \rho u \\ p + \rho u^2 \\ \rho uv \end{pmatrix} \qquad \underline{G} = \begin{pmatrix} \rho v \\ \rho uv \\ p + \rho v^2 \end{pmatrix} \tag{2.2}$$

where

$$p = \frac{(\gamma-1)}{\gamma} \rho [h - \tfrac{1}{2} (u^2 + v^2)] \tag{2.3}$$

and h is total specific enthalpy, assumed constant. We intend to satisfy these equations in an approximation to their integral form

$$\oint (\underline{F}\, dy - \underline{G}\, dx) = 0 \tag{2.4}$$

where the integral is around any arbitrary closed contour. To this end, the plane is divided into cells that are either regularly arranged quadrilaterals (Figure 1a) or unstructured triangles (Figure 1b). In either case, the vertices are numbered, and a fluid state $\underline{u}_i$, where $\underline{u} = (\rho, \rho u, \rho v)$, is assigned to the ith vertex. Ni's scheme for quadrilaterals approximates (2.4) by trapezium rule integration around each cell. This is

$$\underline{D}_{\text{cell}} = \sum_{\text{sides}} [\tfrac{1}{2} (\underline{F}_A + \underline{F}_B) (y_B - y_A) - \tfrac{1}{2} (\underline{G}_A + \underline{G}_B) (x_B - x_A)] \tag{2.5}$$

where the summation is over all sides of the cells, and all differences are taken anticlockwise. Note that D has dimensions of the time derivatives of the actual conserved quantities (not their densities), so that $\underline{D}$ indicates how masses, etc., associated with the points A, B, C, D are to be changed. Different time-marching schemes result from specifying different weights with which the changes are distributed over A, B, C, D. Ni's original recipe [7] reproduced a type of Lax-Wendroff algorithm, and Hall [10] has presented a Runge-Kutta version. Here, however, we are interested only in the steady state which we assume is characterized by the vanishing of $\underline{D}$ for every cell. In practice, this will only happen if the boundary conditions are specified carefully. (For example, on a grid of $n \times n$ cells there will be n^2 equations and $(n+1)^2$ unknowns; hence $2n+1$ boundary conditions must be

prescribed.) Also, the residuals do not in general vanish near a captured shock [11]. This implies that our interest here is chiefly in the accuracy obtained in smooth parts of the flow.

In Jameson's triangular grid scheme [13], the average flux across each line joining two vertices is evaluated as

$$\underline{E}_{AB} = \frac{1}{2} (\underline{F}_A + \underline{F}_B) (y_B - y_A) - \frac{1}{2} (\underline{G}_A + \underline{G}_B) (x_B - x_A). \qquad (2.6)$$

Then masses, etc., proportional to $\underline{E}_{AB}\Delta t$ are added at X and subtracted at Y. When this has been done for all edges in the mesh, then every point has been changed by a net amount proportional to the flux across the perimeter of the polygon formed by all triangles meeting at that point. At the steady state, we again assume that all these flux integrals vanish - due care being taken at the boundary.

It is the ability to characterize steady state solutions in this rather simple way that makes the accuracy of cell-vertex schemes much easier to analyze than Lax-Wendroff schemes where the statement of local equilibrium typically involves nine fluid states and thirty-two mesh coordinates. The statement of equilibrium for a Jameson-type scheme on quadrilaterals involves only five fluid states, but analysis of its accuracy needs twenty-four mesh coordinates.

3. Finite-Difference Analysis

We wish to know how accurately the formula

$$\underline{D}_F = \sum \frac{1}{2}(\underline{F}_A + \underline{F}_B) (y_B - y_A) \qquad (3.1)$$

approximates the integral

$$\underline{I}_F = \oint \underline{F}\, dy \tag{3.2}$$

taken around the same polygonal contour. At this stage, the values of $\underline{F}$ are thought of as point samples, in the spirit of finite difference methods. This is most easily done by assuming that $\underline{F}$ is representable by a Taylor expansion about some arbitrary nearby origin. We consider each side of the polygon in turn. The numerical approximation to the integral is

$$\begin{aligned}\frac{1}{2}(y_B - y_A)(\underline{F}_A + \underline{F}_B) = (y_B - y_A)\Big[\underline{F} &+ \frac{1}{2}(x_A + x_B)\,\underline{F}_x + \frac{1}{2}(y_A + y_B)\,\underline{F}_y \\ &+ \frac{1}{4}(x_A^2 + x_B^2)\,\underline{F}_{xx} + \frac{1}{4}(y_A^2 + y_B^2)\,\underline{F}_{yy} \\ &+ \frac{1}{2}(x_A y_A + x_B y_B)\,\underline{F}_{xy}\Big] \\ &+ 0\,(h^4).\end{aligned} \tag{3.3}$$

The leading terms in the exact integral are found by introducing a local coordinate ξ varying linearly from 0 to 1 over AB, so that a typical point on AB is defined by

$$x(\xi) = \xi\, x_B + (1 - \xi)\, x_A$$

$$y(\xi) = \xi\, y_B + (1 - \xi)\, y_A$$

and

$$\underline{F}(\xi) = \underline{F} + x(\xi)\,\underline{F}_x + y(\xi)\,\underline{F}_y + \frac{1}{2}x^2(\xi)\,\underline{F}_{xx} + x(\xi)y(\xi)\,\underline{F}_{xy} + \frac{1}{2}y^2(\xi)\,\underline{F}_{yy} + O(h^3)\,. \tag{3.4}$$

Inserting these expressions into (3.2) and integrating w.r.t. ξ yields

$$\int_A^B \underline{F}dy = (y_B - y_A)\left[\underline{F} + \frac{1}{2}(x_A + x_B)\,\underline{F}_x + \frac{1}{2}(y_A + y_B)\,\underline{F}_y + \frac{1}{6}(x_A^2 + x_Ax_B + x_B^2)\,\underline{F}_{xx} + \frac{1}{6}(2x_Ay_A + x_Ay_B + x_By_A + 2x_By_B)\,\underline{F}_{xy} + \frac{1}{6}(y_A^2 + y_Ay_B + y_B^2)\,\underline{F}_{yy}\right] + O(h^4)\,. \tag{3.5}$$

Subtracting (3.5) from (3.3) gives the error on AB as

$$\frac{(y_B - y_A)}{12}\left[(x_B - x_A)^2\,\underline{F}_{xx} + 2(x_B - x_A)(y_B - y_A)\underline{F}_{xy} + (y_B - y_A)^2\,\underline{F}_{yy}\right].$$

Hence the total error may be arrived at simply by summing the contribution from all sides. Clearly we can find the error in the $\underline{G}$ integral similarly. The final result is

$$\int \underline{F}\,dy = \sum \overline{\underline{F}}\,\Delta y - E_2\,\underline{F}_{xx} + 2E_3\,\underline{F}_{xy} - E_4\,\underline{F}_{yy} \tag{3.6a}$$

$$\int \underline{G}\,dx = \sum \overline{\underline{G}}\,\Delta x - E_1\,\underline{G}_{xx} + 2E_2\,\underline{G}_{xy} - E_3\,\underline{G}_{yy} \tag{3.6b}$$

where

$$E_1 = \frac{1}{12} \sum (\Delta x)^3$$

$$E_2 = \frac{1}{12} \sum (\Delta x)^2 \Delta y \qquad (3.7)$$

$$E_3 = \frac{1}{12} \sum \Delta x \, (\Delta y)^2$$

$$E_4 = \frac{1}{12} \sum (\Delta y)^3 .$$

It is pleasing that the error constants take these simple forms and useful that there are only four of them. Observe that the quantities we wish to approximate are $O(h^2)$ and that, superficially, the error constants are $O(h^3)$, making the method first-order accurate. However, some cancellation takes place inside the summations in (3.7), which holds out the prospect of better accuracy, depending on geometric properties of the grid which we now investigate.

4. Polygons with Vanishing Error Constants

It is easy to see that any polygon with central symmetry will have E_1 to E_4 identically zero because contributions from opposite sides will vanish. Also, given one error-free polygon, we can form others by permuting the sides and forming mirror images. It is straightforward to show that an error-free polygon remains error-free under rigid rotations. Certain other results are also obtainable.

Theorem 1: A quadrilateral is error-free iff it is a parallelogram.

Proof: For a quadrilateral ABCD, the error constants can be manipulated to read

$$E_1 = (x_A - x_C)(x_B - x_D)(x_A - x_B + x_C - x_D)$$

$$E_2 = 2S(x_A - x_B + x_C - x_D) + (x_A - x_C)(x_B - x_D)(y_A - y_B + y_C - y_D) \tag{4.1}$$

$$E_3 = 2S(y_A - y_B + y_C - y_D) + (y_A - y_C)(y_B - y_D)(x_A - x_B + x_C - x_D)$$

$$E_4 = (y_A - y_C)(y_B - y_D)(y_A - y_B + y_C - y_D)$$

where

$$2S = (x_A - x_C)(y_B - y_D) - (x_B - x_D)(y_A - y_C)$$

and S is the area of the quadrilateral. The only terms which may vanish in these expressions are $(x_A - x_B + x_C - x_D)$, $(y_A - y_B + y_C - y_D)$. These quantities, divided by two, are the components of the vector which joins the midpoints of the two diagonals. Thus E_1 to E_4 vanish iff the diagonals bisect each other, which only happens if the quadrilateral is a parallelogram.

Corollary: No triangle is error-free.

Proof: Since triangles are degenerate quadrilaterals, they are excluded by Theorem 1.

Theorem 2: Any regular n-gon ($n > 3$) is error-free.

Proof: For n even the result is trivial by symmetry. A proof, which includes n odd, follows by considering the polygon in the complex plane. Without loss of generality, one side can be made parallel to the x-axis, and each side is then represented by one of the n^{th} roots of unity, say z_k $(k = 0, \ldots n-1)$ where

$$z_k = \cos \frac{2\pi k}{n} + i \sin \frac{2\pi k}{n}$$

then

$$\sum_k z_k^3 = \sum_k \cos^3 \frac{2\pi k}{n} + 3i \cos^2 \frac{2\pi k}{n} \sin \frac{2\pi k}{n} - 3 \cos \frac{2\pi k}{n} \sin^2 \frac{2\pi k}{n} - i \sin^3 \frac{2\pi k}{n}$$

$$= \sum_k \cos^3 \frac{2\pi k}{n} + 3i \cos^2 \frac{2\pi k}{n} \sin \frac{2\pi k}{n} - 3 \cos \frac{2\pi k}{n} \left(1 - \cos^2 \frac{2\pi k}{n}\right)$$

$$- i \sin \frac{2\pi k}{n} \left(1 - \cos^2 \frac{2\pi k}{n}\right)$$

$$= 4(E_1 + iE_2)$$

$$= \text{(by a similar argument)} - 4(E_3 + iE_4) .$$

But

$$\sum_{k=0}^{k=n-1} z_k^3 = \sum_{k=0}^{k=n-1} z_1^{3k}$$

$$= \frac{z_1^{3n} - 1}{z_1^3 - 1} .$$

The numerator vanishes because $z_1^n = 1$. So the expression equals zero unless the denominator also vanishes; that is, unless n = 3 (when the expression equals 3). So unless $n = 3$, $E_1 = E_2 = E_3 = E_4 = 0$.

For $n > 4$, we can find a variety of asymmetric error-free polygons. The general procedure is to prescribe (n-2) vertices. Then requiring that E_1 to E_4 vanish gives four equations for two unknown coordinate pairs. Unfortunately, these are simultaneous cubic equations for which no systematic solution is apparent. To give a flavor of the possibilities, we consider a pentagon with prescribed vertices at (0,0), (0,1), and (1,0). We maintain symmetry by supposing that an error-free pentagon exists with additional vertices at (1+a,b), (b,1+a). Then we require

$$\sum (\Delta x)^3 = \sum (\Delta y)^3 = 1 - (1+a-b)^3 + a^3 - b^3 = 0 \qquad (4.2)$$

and

$$\sum (\Delta x)^2 \Delta y = \sum (\Delta y^2)\Delta x = ab^2 - (1+a-b)^3 - ba^2 = 0. \qquad (4.3)$$

Condition (4.2) simplifies to

$$3(a-b)(a+1)(b-1) = 0; \qquad (4.4)$$

if $(a-b) = 0$, there are no solutions to (4.3). If $b = 1$, then (4.3) yields

$$a^3 + a^2 - a = 0$$

$$a = 0, \frac{1}{2}(-1 \pm \sqrt{5}),$$

whereas, if $a = -1$ then

$$b^3 - b^2 - b = 0$$

$$b = 0, \frac{1}{2}(1 \pm \sqrt{5}).$$

Although there appear to be six solutions, they actually appear in pairs. In each pair, the sides are permutations of the same set of vectors. The solution to the problem consists of three independent sets of vectors, each of which, by permutation, generates 24 different pentagons, if we allow the given vectors to permute also. However, out of a given set of vectors, only two orderings will produce a convex polygon, that is, those which are monotonically ordered by orientation. Those two are mirror images of each other. The independent convex pentagons derivable from (4.2) and (4.3) are shown in Figure 2. The square is a degenerate case for which one side vanishes.

Error-free polygons can also be constructed by uniting one or more error-free polygons that have edges in common; but, though the construction of error-free polygons has some mathematical interest, it seems unlikely that any practical mesh could be constructed from them, except for completely regular meshes. We turn, therefore, to the more practical question of finding polygons for which the error constants are acceptably small.

5. Polygons with Small Error Constants

The only complete results that have been obtained relate to quadrilaterals, for which the error constants are given by (4.1). The local trunca-

tion error will be $O(h^2)$ provided these expressions are $O(h^4)$. We can clearly identify factors which are $O(h^2)$, and the only possibility for second-order accuracy is that

$$(x_A - x_B + x_C - x_D) = 0\ (h^2), \tag{5.1a}$$

and

$$(y_A - y_B + y_C - y_D) = 0\ (h^2). \tag{5.1b}$$

Although these conditions are not met by arbitrary quadrilaterals, they are met by quadrilaterals which are produced as part of an analytic grid. Suppose we have grid generating functions

$$x = x\ (\xi, \eta)$$

$$y = y\ (\xi, \eta)$$

and the mesh points are the intersections of $\xi = m\Delta\xi$, $\eta = n\Delta\eta$, for integer values of m, n. Then, if the mesh is systematically refined, $\Delta\xi$, $\Delta\eta$ tend to zero, and

$$(x_A - x_B + x_C - x_D) + \frac{\partial^2 x}{\partial\xi\partial\eta}\Delta\xi\partial\eta = 0\ (h^2) \tag{5.2a}$$

$$(y_A - y_B + y_C - y_D) + \frac{\partial^2 y}{\partial\zeta\partial\eta}\Delta\zeta\Delta\eta = O(h^2) \tag{5.2b}$$

provided the cross-derivatives are not large.

Note that since the error terms involve only the local intrinsic geometry of each cell, neighboring cells may be of markedly different shape, size, or orientation. That statement cannot be made for finite-volume schemes

[5,11]. Indeed, the local quality of cell-vertex schemes makes them second-order accurate on grids generated more straightforwardly than those described above. Suppose a coarse grid is determined arbitrarily, and fine grids are constructed from it by repeatedly bisecting the cell edges. Within each of the original cells, PQRS, there is a mapping defined by

$$x = (1-\xi)(1-\eta)\, x_P + \xi(1-\eta)x_Q + \xi\eta\, x_R + (1-\xi)\,\eta x_S \tag{5.3a}$$

$$y = (1-\xi)(1-\eta)\, y_P + \xi(1-\eta)y_Q + \xi\eta\, y_R + (1-\xi)\,\eta y_S \tag{5.3b}$$

which meets the conditions (5.2).

Related results have been found by Paisley [11], who finds that in the cell-vertex method, it is allowable to perturb a rectangular mesh by $O(h^2)$ whereas with Jameson's [4] scheme, the allowable perturbation is only $O(h^3)$.

6. A Finite-Element Approach

As mentioned in the introduction, the schemes under study have been described elsewhere as finite element schemes. Whether this is justifiable or not, there is one objection that can be removed. This objection is that the formula

$$\int (\underline{F}\, dy - \underline{G}\, dx) = \frac{1}{2} \sum (\underline{F}_i + \underline{F}_{i+1})(y_{i+1} - y_i) - (\underline{G}_i + \underline{G}_{i+1})(x_{i+1} - x_i)$$

is obtained by integrating over each triangular (quadrilateral) element assuming a linear (bilinear) distribution for both $\underline{F}$ and $\underline{G}$, which is incon-

sistent because there is a nonlinear functional relationship between $\underline{F}$ and $\underline{G}$. A consistent finite-element model can be derived by assuming that the vector $\underline{w}$ varies linearly (bilinearly) over the elements, where

$$\underline{w} = \rho^{1/2} \begin{pmatrix} 1 \\ u \\ v \end{pmatrix} . \tag{6.2}$$

These variables were introduced by the author to facilitate the construction of an approximate Riemann solver [14]. They have the property that every component of $\underline{u}$, $\underline{F}$, $\underline{G}$ is bilinear in the components of $\underline{w}$. Thus

$$\underline{F} = \begin{vmatrix} w_1 w_2 \\ \frac{\gamma-1}{2\gamma} h w_1^2 + \frac{\gamma+1}{2\gamma} w_2^2 - \frac{\gamma-1}{2\gamma} w_3^2 \\ w_2 w_3 \end{vmatrix} \tag{6.3}$$

where h is a constant for steady flow, equal to the specific total enthalpy. In computing a typical term of (6.1) such as

$$I^{AB} = \int_A^B \underline{F}\, dy$$

there will be subterms of the form

$$I^{AB}_{i,j} = \int_A^B w_i w_j \, dy . \tag{6.4}$$

The consistent evaluation of this term is

$$I^{AB}_{i,j} = (y_B - y_A) \int_0^1 [\xi\, w_{iB} + (1-\xi) w_{iA}]\, [\xi w_{jB} + (1-\xi) w_{jA}]\, d\zeta$$

$$= (y_B - y_A)\,[2w_{iB}w_{jB} + w_{iA}w_{jB} + w_{iB}w_{jA} + 2w_{iA}w_{jA}]$$

$$= \frac{1}{2}(y_B - y_A)\,[w_{iB}w_{jB} + w_{iA}w_{jA}]$$

$$- \frac{1}{6}(y_B - y_A)\,(w_{iB} - w_{iA})\,(w_{jB} - w_{jA}). \qquad (6.5)$$

The first term contributes the 'naive' approximation $\frac{1}{2}(y_B - y_A)(\underline{F}_B + \underline{F}_A)$; the second term is part of a correction that makes the approximation self-consistent. The leading contributions to it are due to first derivatives of $\underline{w}$. The correction term in (6.5) is, to leading order,

$$\frac{1}{6}(y_B - y_A)^3 w_{iy}w_{jy} + \frac{1}{6}(y_B - y_A)^2(x_B - x_A)\,[w_{iy}w_{jx} + w_{ix}w_{jy}]$$

$$+ \frac{1}{6}(y_B - y_A)\,(x_B - x_A)^2 w_{ix}w_{jx}.$$

When we sum such terms over every side of the polygon, expressions arise proportional to the constants E_1, E_2, E_3, E_4 given by equations (3.7). Where these error constants are small enough, the error due to inconsistency is negligible, and both the consistent and inconsistent formulae approximate the flux integrals to $O(h^2)$.

7. An Integral Formulation of Axisymmetric Flow

Flow which is identical in every plane through some axis of symmetry is governed by differential equations that can be written in either of the forms

$$\underline{u}_t + \underline{F}_x + \underline{G}_r = (v/r)\,\underline{u} \tag{7.1}$$

or

$$(r\underline{u})_t + (r\underline{F})_x + (r\,\underline{G})_r = \underline{p} \tag{7.2}$$

where $\underline{u}$, $\underline{F}$, $\underline{G}$ are the usual conserved quantities in two-dimensional flow, except that r is now a radial coordinate, and v a radial velocity. Here $\underline{p}$ is the vector $(0, 0, p, 0)^T$.

As a basis for numerical work, (7.1) is tempting because it requires only slight modification to a two-dimensional code. However, (7.2) is a better basis for shock-capturing because it expresses conservation more exactly. To see this, imagine that we are performing a truly three-dimensional computation, using the same grid in every axial plane, so that each 3-D cell is a 2-D cell rotated through some angle θ with respect to the axis (Figure 3). The exact angle does not matter, so long as we avoid the extremes 0 and 2π.

If we make a flux balance on such a control volume, the contributions from the four faces which do not lie in the radial planes can be evaluated analytically, by integrating with respect to the angle. The result is

$$\frac{\partial}{\partial t}\iint_{\Omega} r\,\underline{u}\,dA - \partial_{\Omega}\int (r\underline{F}\,dr - r\,\underline{G}dx) - \iint_{\Omega} \underline{p}\,dA = 0 \tag{7.3}$$

where Ω is the interior of the 2-D cell, and $\partial\Omega$ its boundary.

In order to check that a proposed solution was conservative (and hence a correct weak solution), we would check that all such integral equations were satisfied. A numerical method which imposes this as a constraint will be a correct shock-capturing method. In this way, we can give an interpretation to conservation of "radial momentum" via the third equation in (7.3).

Equation (7.3) can be the basis for extending to axisymmetric flow either of the cell-vertex methods under discussion. In Ni's scheme, one integrates the quantities $r\underline{F}$, $r\underline{G}$ around quadrilaterals; in Jameson's scheme, the quantity $r(\underline{F}\Delta y - \underline{G}\Delta x)$ is evaluated for each side and used to update the adjoining vertices. The problem we now address is how to evaluate these things numerically.

8. Error Analysis for the Axisymmetric Methods

In either method, the central ingredient is an expression of the form

$$\int_A^B r\,\underline{F}\,dr \quad \text{or} \quad \int_A^B r\,\underline{G}\,dx.$$

Consider the first of these. Two plausible computational formulae are

$$I^1_{AB} = \frac{1}{2}(r_B - r_A)\,[r_A F_A + r_B F_B] \tag{8.1}$$

$$I^2_{AB} = \frac{1}{4}(r_B - r_A)\,(r_A + r_B)\,[F_A + F_B]. \tag{8.2}$$

As in the two-dimensional case, we find what the exact value of the integral should be in terms of a Taylor expansion about an arbitrary nearby point. The result is

$$I_{AB} = (r_B - r_A)\left[\frac{1}{2}(r_B + r_A)\underline{F} + \frac{1}{6}(2r_Ax_A + r_Ax_B + r_Bx_A + 2r_Bx_B)\underline{F}_x\right.$$

$$+ \frac{1}{3}(r_A^2 + r_Ar_B + r_B^2)\underline{F}_r$$

$$+ \frac{1}{24}(3r_Ax_A^2 + 2r_Ax_Ax_B + r_Ax_B^2 + r_Bx_A^2 + 2r_Bx_Ax_B + 3r_Bx_B^2)\underline{F}_{xx} \qquad (8.3)$$

$$+ \frac{1}{12}(3r_A^2x_A + 2r_Ar_Bx_A + r_B^2x_A + r_B^2x_A + r_A^2r_B + 2r_Ar_Bx_B + 3r_B^2x_B)\,\underline{F}_{xr}$$

$$\left. + \frac{1}{8}(r_A^3 + r_A^2r_B + r_Ar_B^2 + r_B^3)\,\underline{F}_{rr}\right] + \ldots .$$

If we make similar expansions for the approximations (8.1), (8.2), and subtract from them (8.3), we find error estimates as follows.

$$I_{AB}^1 - I_{AB} = (r_B-r_A)\left[\frac{1}{6}(r_B-r_A)(x_B-x_A)\underline{F}_x + \frac{1}{6}(r_B - r_A)^2\underline{F}_r\right.$$

$$- \frac{1}{24}(x_B-x_A)(3r_Ax_A + r_Ax_B - r_Bx_A - 3r_Bx_B)\,\underline{F}_{xx} \qquad (8.4)$$

$$- \frac{1}{12}(r_B-r_A)\,(3r_Ax_A - r_Ax_B + r_Bn_A - 3r_Bx_B)\,\underline{F}_{xr}$$

$$\left. + \frac{1}{8}(r_B-r_A)(r_B^2 - r_A^2)\,\underline{F}_{rr}\right] + \ldots$$

$$I_{AB}^2 - I_{AB} = (r_B-r_A)\left[-\frac{1}{12}(r_B-r_A)(x_B-x_A)\,\underline{F}_x - \frac{1}{12}(r_B-r_A)^2\,\underline{F}_r\right.$$

$$+ \frac{1}{12}(x_B-x_A)\,(r_Ax_B - r_Bx_A)\,\underline{F}_{xx} \qquad (8.5)$$

$$\left. + \frac{1}{12}(r_B-r_A)\,(r_Ax_B - r_Bx_A)\,\underline{F}_{xr}\right] + \ldots$$

Combining terms for a particular polygonal control volume, we obtain the following equations relating the exact integral to the approximations (8.1), (8.2).

$$\int_A^B r\,\underline{F}\,dr = \tfrac{1}{2}\sum (r_B - r_A)\,[r_A\underline{F}_A + r_B\,\underline{F}_B] + 2E_3\,\underline{F}_x + 2E_4\,\underline{F}_r + \ldots \qquad (8.6)$$

$$= \tfrac{1}{4}\sum (r_B^2 - r_A^2)\,[\underline{F}_A + \underline{F}_B] - E_3\underline{F}_x - E_4\underline{F}_r + \ldots \qquad (8.7)$$

wherein we again find the error constants defined in (3.7). At first sight, this is a satisfactory result showing that the errors are $O(h^4)$ on a smooth grid. However, the quantity being approximated is $\iint r\underline{F}_x\,dA$, which is $O(rh^2)$. The problem is that, near the axis, we find cells for which r is $O(h)$, and the error terms are $O(h)$ relative to the true values. On a non-smooth mesh, they are even $O(1)$.

We observe from (8.6) and (8.7) that these particular errors could be eliminated by choosing the linear combination

$$I_{AB}^3 = \frac{1}{3}\,I_{AB}^1 + \frac{2}{3}\,I_{AB}^2 = \frac{1}{6}\,(r_B - r_A)\,[2r_A\,\underline{F}_A + r_A\,\underline{F}_B + r_B\,\underline{F}_A + 2r_B\,\underline{F}_B]. \qquad (8.8)$$

Note that this is the combination obtained if we assume that r, $\underline{F}$, both vary linearly along AB, and then integrate exactly. The error analysis for a single side now gives

$$I_{AB}^3 - I_{AB} = (r_B - r_A)\,(r_B + r_A)\,[\frac{1}{24}\,(x_B - x_A)^2\underline{F}_{xx} + \frac{1}{12}(x_B - x_A)(r_B - r_A)\,\underline{F}_{xr} + \frac{1}{24}\,(r_B - r_A)^2\,\underline{F}_{rr}]. \qquad (8.9)$$

Therefore, the total error around a particular polygon is

$$\sum I_{AB}^3 - \int r \underline{F} ds = \frac{1}{12} \underline{F}_{xx} \sum \bar{r}(\Delta x)^2 \Delta r + \frac{1}{6} \underline{F}_{xr} \sum \bar{r} (\Delta x) (\Delta r)^2 + \frac{1}{12} \underline{F}_{rr} \sum \bar{r} (\Delta r)^3 + \ldots \quad . \tag{8.10}$$

The analysis is now identical to the two-dimensional case except for the appearance of the mean radii $(\bar{r})$ in every term. These factors, however, complicate matters considerably. For example, it is no longer true that a regular polygon has vanishing error constants because contributions from opposite sides no longer cancel in general. To put the error constants into forms which make their order of magnitude self-evident needs considerable manipulation, which has only been carried out for quadrilaterals. The easiest term to analyze then is

$$\begin{aligned}
\sum (r_i + r_{i+1}) (r_{i+1} - r_i)^3 &= r_B^4 - 2r_B^3 r_A + 2r_B r_A^3 - r_A^4 \\
&\quad + r_C^4 - 2r_C^3 r_B + 2r_C r_B^3 - r_B^4 \\
&\quad + r_D^4 - 2r_D^3 r_C + 2r_D r_C^3 - r_C^4 \\
&\quad + r_A^4 - 2r_A^3 r_D + 2r_A r_D^3 - r_D^4 \\
&= 2r_A^3(r_B - r_D) + 2r_B^3(r_C - r_A) + 2r_C^3(r_D - r_B) + 2r_D^3(r_A - r_C) \\
&= 2(r_A - r_C)(r_D^3 - r_B^3) - 2(r_D - r_B)(r_A^3 - r_C^3)
\end{aligned}$$

$$= 2(r_A - r_C)\,(r_D - r_B)\,(r_D^2 + r_D r_B + r_B^2 - r_A^2 - r_A r_C - r_C^2)$$

$$= 2(r_A - r_C)(r_D - r_B)\left[\tfrac{3}{4}\,(r_D + r_B)^2 + \tfrac{1}{4}\,(r_D - r_B)^2 - \tfrac{3}{4}\,(r_A + r_C)^2 - \tfrac{1}{4}\,(r_A - r_C)^2\right]$$

$$= \tfrac{3}{2}\,(r_A - r_C)\,(r_B - r_D)\,(r_A + r_B + r_C + r_D)\,(r_A - r_B + r_C - r_D)$$

$$+ \tfrac{1}{2}\,(r_A - r_C)\,(r_B - r_D)\,(r_A + r_B - r_C - r_D)\,(r_A - r_B - r_C + r_D). \qquad (8.11)$$

The first term is $O(rh^4)$ on grids which are smooth in the sense of the previous discussion; it is $O(rh^3)$ on non-smooth grids. The second term appears to be $O(h^4)$. That it shall be $O(rh^4)$ imposes a natural condition on the grid near the axis. If the cell nearest the axis has one side on the axis, then it can be shown that one of the factors $(r_A + r_B - r_C - r_D)$, $(r_A - r_B - r_C + r_D)$ is $O(h)$; the other is $O(rh)$--which one is which depends on the labelling. It is assumed that this cell is also smooth in the same sense as the others.

We will omit details of the calculations that show the other terms in (8.10) to be $O(rh^4)$, simply exhibiting the final rearrangements. We find

$$\sum \bar{r}(\Delta x)^2 \Delta r = (x_B - x_D)\,(x_A - x_C)\,(r_A^2 - r_B^2 + r_C^2 - r_D^2)$$

$$+ (x_A - x_C)\,(r_B^2 - r_D^2)\,(x_A - x_B + x_C - x_D) \qquad (8.12)$$

$$+ (x_B - x_D)\,(r_A^2 - r_C^2)\,(x_A - x_B + x_C - x_D).$$

Here the last two terms are $O(rh^4)$ on any smooth grid, and the first one is so if the axis is included. Also, with great patience, we can obtain:

$$\begin{aligned}\sum \bar{r}(\Delta x)(\Delta r)^2 = &\frac{1}{2}(r_A + r_B + r_C + r_D)(r_B - r_D)(r_A - r_C)(x_A - x_B + x_C - x_D)\\ &+ S\,(r_A + r_B + r_C + r_D)(r_A - r_B + r_C - r_D)\\ &+ \frac{1}{2} S\,(r_A + r_B - r_C - r_D)(r_A - r_B - r_C + r_D)\\ &+ \frac{1}{2}(r_A - r_B + r_C - r_D)^2[(r_A - r_C)(x_B - x_D) + (r_B - r_D)(x_A - x_C)]\end{aligned} \tag{8.13}$$

where S is the cell area.

On smooth grids, the first three lines are $O(rh^4)$; the fourth is $O(h^6)$.

Now we turn to the terms involving $\underline{G}$ and $\underline{p}$ in equation (8.3). Both of these terms are $O(h^2)$, but near the axis they almost cancel so the requirement for accuracy is the same as for the other terms. A straightforward evaluation of $\iint \underline{p}\, dA$ cannot avoid errors $O(h^4)$ so some subtlety is needed.

Integration by parts shows that

$$\iint_\Omega \underline{p}\, dA = \int_{\partial\Omega} r\, \underline{p}\, dx - \iint_\Omega r \frac{\partial p}{\partial r} \cdot dA, \tag{8.14}$$

and we can use this to rewrite the terms in $\underline{G}$ and $\underline{p}$ as

$$\int_{\partial\Omega} r\, \underline{G}\, dx - \iint_\Omega \underline{p}\, dA = \int_{\partial\Omega} r\,(\underline{G} - p)\, dx + \iint_\Omega r \frac{\partial p}{\partial r}\, dA \tag{8.15}$$

where both terms on the RHS are of order (rh^2). Now we can evaluate the contour integral by the methods just discussed; the error terms will be

$$\frac{1}{12}(\underline{G} - \underline{p})_{xx} \sum \bar{r}(\Delta x)^3 + \frac{1}{6}(\underline{G} - \underline{p})_{xr} \sum \bar{r}(\Delta x)^2 \Delta r + \frac{1}{12}(\underline{G} - \underline{p})_{rr} \sum \bar{r} \Delta x (\Delta r)^2. \tag{8.16}$$

The summations multiplying $\underline{G}_{xr}$, $\underline{G}_{rr}$ have already been shown to be $O(rh^4)$. The first summation can be evaluated as

$$\begin{aligned}\sum \bar{r}(\Delta x)^3 = &-\frac{3}{2}(r_A + r_B + r_C + r_D)(x_A - x_C)(x_B - x_D)(x_A - x_B + x_C - x_D) \\ &- \frac{1}{4}[(r_A - r_C)(x_B - x_D) + (r_B - r_D)(x_A - x_C)] \\ &(x_A + x_B - x_C - x_D)(x_A - x_B - x_C + x_D) \\ &+ \frac{1}{2} S[3(x_A - x_B + x_C - x_D)^2 + (x_A - x_B - x_C + x_D)^2 \\ &+ (x_A + x_B - x_C - x_D)^2].\end{aligned} \tag{8.17}$$

Every term in this expression can be justified as $O(rh^4)$ on a smooth mesh, except for the third line. Here S is $O(h^2)$ and the first term inside the bracket is $O(h^4)$, but of the two remaining terms, one will be $O(r^2h^2)$ and the other $O(h^2)$. Thus, the overall order of the expression must be h^4. However, this does not destroy the second-order accuracy of the scheme near the axis, because in that region $(\underline{G} - \underline{p})_{xx}$ is $O(r)$ so that all contributions to (8.16) are actually $O(rh^4)$.

Lastly, we have to evaluate

$$\iint_{\Omega} r \frac{\partial p}{\partial r} \, dA \, . \tag{8.18}$$

A formula for this can be found using finite element techniques, if the gradient is rewritten as

$$\frac{\partial p}{\partial r} = \frac{1}{J} \left(\frac{\partial p}{\partial \xi} \cdot \frac{\partial x}{\partial \eta} - \frac{\partial p}{\partial \eta} \cdot \frac{\partial x}{\partial \xi} \right)$$

where J is the Jacobian of the transformation $(\xi, \eta) \to (x, y)$. Since we also have $dA = J \, d\xi \, dy$, (8.18) can be found straightforwardly. The result is

$$\iint_{\Omega} r \frac{\partial p}{\partial r} \, dA$$

$$= \frac{(x_B - x_D)}{24} [p_A(4r_A + 3r_B + 2r_C + 3r_D) - p_C(2r_A + 3r_B + 4r_C + 3r_D)]$$

$$- \frac{(x_A - x_C)}{24} [p_B(3r_A + 4r_B + 3r_C + 2r_D) - p_D(3r_A + 2r_B + 3r_C + 4r_D)]$$

$$+ \frac{(r_B - r_D)}{24} [p_A(x_B + x_D - 2x_C) - p_C(x_B + x_D - 2x_A)]$$

$$- \frac{(r_A - r_C)}{24} [p_B(x_A + x_C - 2x_D) - p_D(x_A + x_C - 2x_B)]. \tag{8.19}$$

The error term turns out to be

$$\frac{1}{8} (r_A + r_B + r_C - r_D)(x_A - x_B + x_C - x_D)[(x_A - x_C)(x_B - x_D)p_{xx} +$$

$$(r_A - r_C)\,(r_B - r_D)\,p_{rr}]$$

$$+ \frac{1}{24}\,[(r_A + r_B + r_C + r_D)\{2S(x_A - x_B + x_C - x_D) +$$

$$+ (x_B - x_D)\,(x_A - x_C)\,(r_A - r_B + r_C - r_D)\}$$

$$+ (r_A - r_C)\,(r_B - r_D)\,(x_A - x_B - x_C + x_D)\,(x_A + x_B - x_C - x_D)]\,p_{xr}. \tag{8.20}$$

All terms in this expression are $O(rh^4)$ provided the grid is smooth and contains the axis. The scheme which has emerged, although more cumbersome than one would hope for, is the unique cell vertex scheme retaining second-order accuracy in axisymmetric flow. It may be noted that it has also one property commonly demanded of a numerical code. It is satisfied identically by uniform flow parallel to the axis. For such a flow, $\underline{F}$ is a constant, ($\underline{G}$ - $\underline{p}$) vanishes, and $\partial p/\partial r$ vanishes. Under these circumstances, all contributions to the balance equations vanish identically.

The expressions which have been found as approximations, in effect, to $\partial \underline{F}/\partial x$ and $\partial \underline{G}/\partial r$ have been derived by other authors from other considerations. Margolin and Adams [15], in the context of a Lagrangian scheme, sought numerical approximations that would make the equation

$$\frac{1}{V}\frac{dV}{dt} = \text{div}\ \underline{u} \tag{8.21}$$

an identity at the discrete level. Here V is the volume of a moving parcel of fluid. The unique solution to this problem gave the differentiation operators derived here. Margolin and Adams report greatly improved accuracy in their computations.

The same operators were also obtained by Holm et al. [18] as the unique operators to preserve in the discrete formulation certain Hamiltonian properties of the differential equations.

If the scheme were to be used in practice, it may be noted that some simplifications of the expressions are possible, at least for quadrilateral control volumes. The terms involving $\underline{F}$ can be made more compact by rearrangement. The terms involving p in (8.19) can be used partly to cancel the terms in $(\underline{G} - \underline{p})$. What emerges from this is the following, which we claim is the simplest version of the unique formula

$$
\begin{aligned}
&\tfrac{1}{6}(r_B - r_D)\ [(r_D + r_A + r_B)\,\underline{F}_A - (r_B + r_C + r_D)\,\underline{F}_C] \\
&- \tfrac{1}{6}(r_A - r_C)\ [(r_A + r_B + r_C)\,\underline{F}_B - (r_C + r_D + r_A)\,\underline{F}_D] \\
&- \tfrac{1}{6}(x_B - x_A)\ [2r_A\,\underline{G}_A + r_A\underline{G}_B + r_B\,\underline{G}_A + 2r_B\,\underline{G}_B] \\
&- \tfrac{1}{6}(x_C - x_B)\ [2r_B\,\underline{G}_B + r_B\,\underline{G}_C + r_C\,\underline{G}_B + 2r_C\underline{G}_C] \\
&- \tfrac{1}{6}(x_D - x_C)\ [2r_C\,\underline{G}_C + r_C\,\underline{G}_D + r_D\,\underline{G}_C + 2r_D\,\underline{G}_D] \qquad (8.22) \\
&- \tfrac{1}{6}(x_A - x_D)\ [2r_D\,\underline{G}_D + r_D\,\underline{G}_A + r_A\,\underline{G}_D + 2r_A\,\underline{G}_A] \\
&+ \tfrac{S}{4}(\underline{p}_A + \underline{p}_B + \underline{p}_C + \underline{p}_C) \\
&+ \tfrac{1}{24}(\underline{p}_A - \underline{p}_C)\ [(x_B - x_D)(r_A + r_C) - (r_B - r_D)(x_A + x_C)] \\
&- \tfrac{1}{24}(\underline{p}_B - \underline{p}_D)\ [(x_A - x_C)(r_B + r_D) - (r_A - r_C)(x_B + x_D)] = 0\,.
\end{aligned}
$$

A striking feature is that the approximations to $\int r \underline{G}\, dx$ and $\iint \underline{p}\, dA$ are precisely those that would have been obtained by finite-element integrations assuming bilinear variations for $\underline{G}$ and $\underline{p}$. However, neither of those terms individually is second-order accurate. The combination is, given suitable conditions on the grid.

9. Conclusions

The cell vertex schemes studied in this paper have been claimed as second-order accurate on arbitrary grids. Certainly the results show an impressive convergence as the grids are refined [10]. However, we have shown that on arbitrary grids, the local truncation error may be first-order. Explicit error constants associated with grid geometry have been derived. These indicate what sort of cell shapes to avoid and could also be used as part of a mesh refinement strategy.

The extension to axisymmetric flow has been made, and it seems harder to achieve accuracy then. The unique formula which retains second-order accuracy near the axis has been derived. However, the extension to fully three-dimensional schemes is an extremely difficult piece of algebra which has not yet been attempted.

REFERENCES

[1] A. Rizzi, M. Inouye, "A time-split finite-volume technique for three-dimensional blunt-body flow." AIAA Journal, No. 11, 1973, pp. 1478-1485.

[2] P. D. Lax, B. Wendroff, "Difference schemes for hyperbolic equations with high order of accuracy." Comm. Pure and Appl. Math., Vol. 17, 1964, pp. 381-398.

[3] P. D. Lax, "Weak solutions of nonlinear hyperbolic equations and their numerical computation." Comm. Pure and Appl. Math., Vol. 7, 1954, pp. 159-193.

[4] A. Jameson, W. Schmidt, E. Turkel, "Numerical solutions of the Euler equations by finite volume methods using Runge-Kutta time-marching schemes." AIAA paper 81-1259, 1981.

[5] E. Turkel, "Accuracy of schemes with nonuniform meshes for compressible fluid flows." Appl. Numer. Math., in press.

[6] E. Turkel, S. Yaniv, U. Landau, "Accuracy of schemes for the Euler Equations with nonuniform meshes." ICASE Report No. 85-59, 1985. Also AIAA paper 86-0341.

[7] R-H. Ni, "A multiple-grid scheme for solving the Euler equations." AIAA Journal, Vol. 20, No. 11, 1982, pp. 1565-1571.

[8] R. L. Davis, R-H. Ni, W. W. Bowley, "Prediction of compressible laminar viscous flows using time-marching control volume and multiple grid technique." AIAA Journal, Vol. 22, No. 11, 1984, pp. 1573-1581.

[9] R. Lohner, K. Morgan, J. Peraire, O. C. Zienkiewiez, "Finite-element methods for high-speed flows." AIAA paper 85-1531-CP, 1985.

[10] M. G. Hall, "Cell vertex multigrid schemes for solution of the Euler equations." In Numerical Methods for Fluid Dynamics II, K. W. Morton, M. J. Banes (eds.), Oxford University Press, 1986, pp. 303-345.

[11] M. F. Paisley, "A comparison of cell centre and cell vertex schemes for the steady Euler equations." Oxford University Computing Laboratory, Numerical Analysis Group, Report 86/1, 1986.

[12] K. W. Morton, M. F. Paisley, "On the cell-centre and cell-vertex approaches to the steady Euler equations and the use of shock fitting." 10th Int. Conf. Num. Meth. Fluid Dyn., Beijing, 1986.

[13] A. Jameson, T. J. Baker, N. P. Weatherill, "Calculation of inviscid transonic flow over a complete aircraft." AIAA paper 86-0103, 1986.

[14] P. L. Roe, "Approximate Riemann solvers, parameter vectors and difference schemes." J. Comput. Phys., Vol. 43, 1981, pp. 357-372.

[15] L. F. Margolin, T. F. Adams, "Spatial differencing for finite difference codes." Report LA-10249, Los Alamos National Laboratory, January 1985.

[16] D. D. Holm, B. A. Kupershmidt, C. D. Levermore, "Hamiltonian differencing of fluid dynamics." Advances in Applied Mathematics, Vol. 6, 1985, pp. 52-84.

APPENDIX

Some Properties of the Jameson Formula

At convergence, Jameson's scheme for triangles [13] satisfies

$$\frac{1}{2}\sum_i (F_i + F_{i+1})(y_{i+1} - y_i) - \frac{1}{2}\sum_i (G_i + G_{i+1})(x_{i+1} - x_i) = 0 \qquad (A.1)$$

around the perimeter of every polygon formed from the set of triangles meeting at a common vertex. This has been presented as a set of flux balance equations around an overlapping set of control volumes. A straightforward rearrangement of (A.1) is

$$\frac{1}{2}\sum_i \underline{F}_i(y_{i+1} - y_{i-1}) - \frac{1}{2}\sum_i \underline{G}_i(x_{i+1} - x_{i-1}) = 0. \qquad (A.2)$$

Now $\sum (y_{i+1} - y_{i-1}) = 0$, because if the polygon has an odd number of sides, we travel twice round its perimeter to rearrive at our starting vertex, and with even sides there are two closed polygonal paths. Therefore, we can add arbitrary constants to the $\underline{F}_i$, $\underline{G}_i$. Let us choose $\underline{F}_0$, $\underline{G}_0$ which are the values at the common vertex (Figure 1b). Rewrite (A.2) as

$$\sum_i \frac{1}{2}(\underline{F}_0 + \underline{F}_i)\frac{1}{3}(y_{i+1} - y_{i-1}) - \sum_i \frac{1}{2}(\underline{G}_0 + \underline{G}_i)\frac{1}{3}(x_{i+1} - x_{i-1}) = 0. \qquad (A.3)$$

The reason for the factors $\frac{1}{3}$ is shown in Figure 4, where P, Q are the controids of OABS, OBC. Then

$$x_P - x_Q = \frac{1}{3}(x_O + x_A + x_B) - \frac{1}{3}(x_O + x_B + x_C) = \frac{1}{3}(x_A - x_B).$$

So (A.3) can be interpreted as the flux balance around non-overlapping control volumes whose edges join the centroids. This interpretation leads to a dual form of the algorithm as follows.

Scheme II

For all edges MN in the mesh, compute

$$\frac{1}{2}\,(\underline{F}_M + \underline{F}_N)\,(y_S - y_T) - \frac{1}{2}\,(\underline{G}_M + \underline{G}_N)\,(x_S - x_T)$$

where S, T are the other vertices of the triangles adjacent to MN, and use this flux to update M, N.

This has an identical outcome to the standard scheme, which we repeat for contrast.

Scheme I

For all edges MN in the mesh, compute

$$\frac{1}{2}\,(\underline{F}_M + \underline{F}_N)\,(y_M - y_N) - \frac{1}{2}\,(\underline{G}_M + \underline{G}_N)\,(x_M - x_N)$$

and use this flux to update S, T.

Indeed, there are two more possibilities, both of which will also yield the same results at convergence.

Scheme III

For all edges MN in the mesh, compute

$$\frac{1}{2}(\underline{F}_S + \underline{F}_T)(y_S - y_T) - \frac{1}{2}(\underline{G}_S + \underline{G}_T)(x_S - x_T)$$

and use this flux to update M, N.

Scheme IV

For all edges MN in the mesh, compute

$$\frac{1}{2}(\underline{F}_S + F_T)(y_M - y_N) - \frac{1}{2}(\underline{G}_S + \underline{G}_T)(x_M - x_N)$$

and use this flux to update S, T.

Given the interpretation that $\underline{u}$ is piecewise linear within each triangle, one is tempted to look for control volumes allowing a more accurate integration. For example (Figure 5), we may consider the control volume formed by joining the centroids of each triangle to the center of each side. Along PI the value of $\underline{F}$, say, varies linearly from $\frac{1}{2}(\underline{F}_O + \underline{F}_B)$ to $\frac{1}{3}(\underline{F}_O + \underline{F}_A + \underline{F}_B)$ with average value $\frac{1}{12}(5\underline{F}_O + 2\underline{F}_A + 5\underline{F}_B)$. (In view of the discussion in Section 6, we neglect the nonlinear variations of $\underline{F}$.) Some algebra will show that this does nothing more than reproduce equations (A.1) or (A.3). This result is obvious if we think of integrating $\underline{F}_x$ over the area of the control volumes. Within OAB, $\underline{F}_x$ is a constant and the area of OJPI is one-third that of OAB.

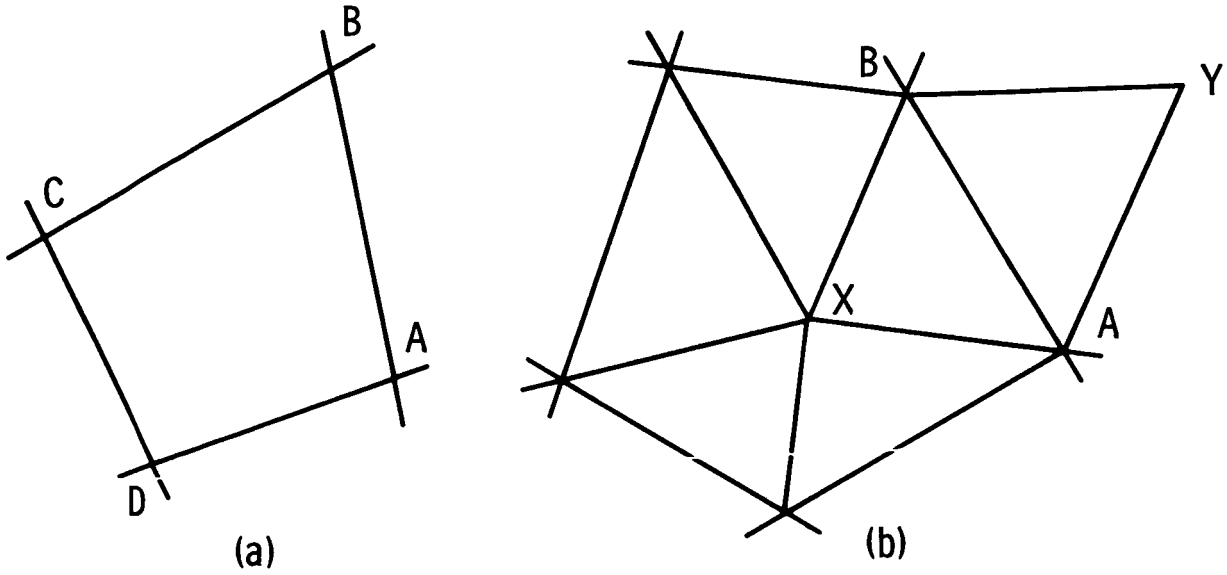

Figure 1. (a) Part of a structured quadrilateral mesh.

(b) Part of an unstructured triangular mesh.

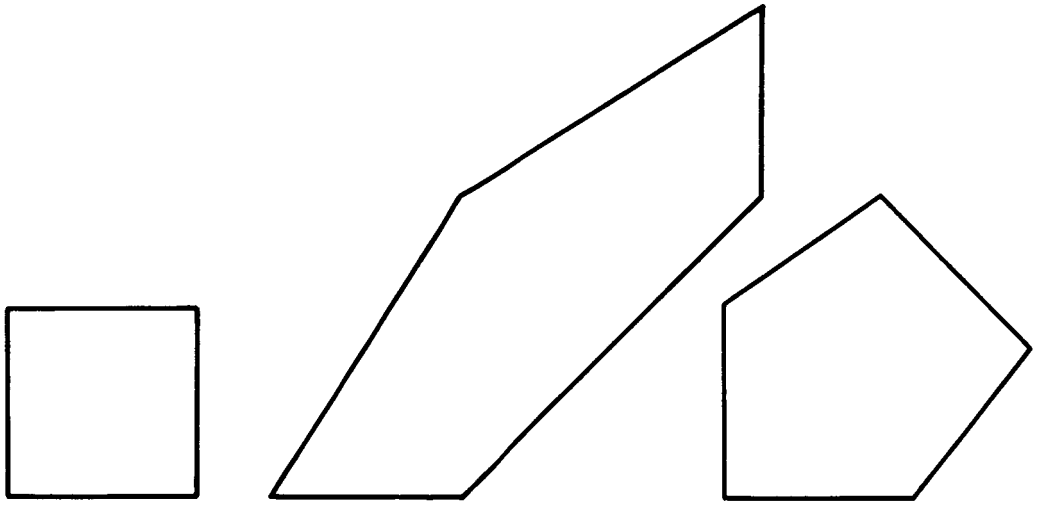

Figure 2. Examples of polygons with zero error constants.

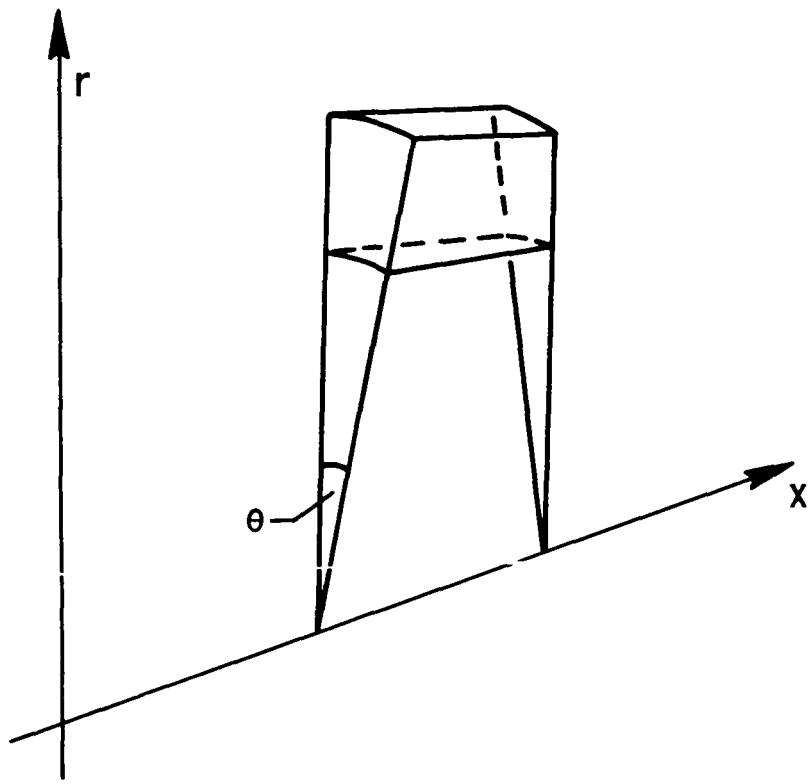

Figure 3. A computational cell partly rotated about the axis.

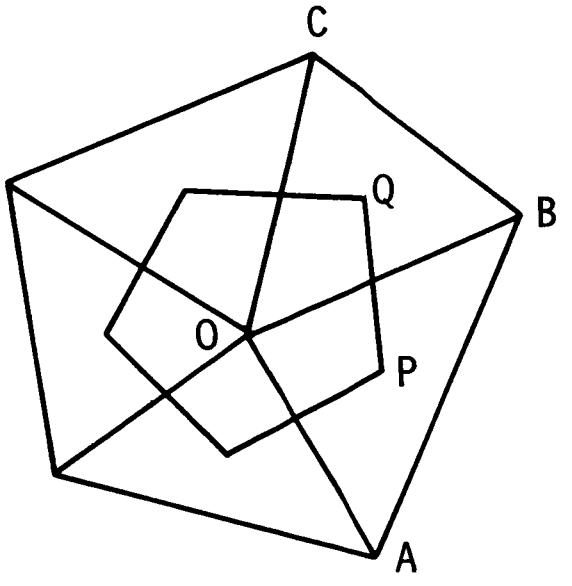

Figure 4. Alternative control volume for Jameson's scheme.

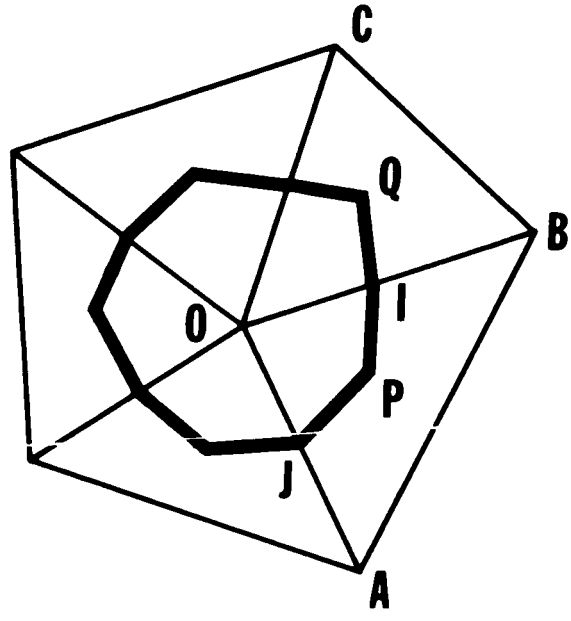

Figure 5. Control volume using cell bisectors.

Standard Bibliographic Page

1. Report No. NASA CR-178235 ICASE Report No. 87-6	2. Government Accession No.	3. Recipient's Catalog No.
4. Title and Subtitle ERROR ESTIMATES FOR CELL-VERTEX SOLUTIONS OF THE COMPRESSIBLE EULER EQUATIONS		5. Report Date January 1987 6. Performing Organization Code
7. Author(s) P. L. Roe		8. Performing Organization Report No. 87-6
9. Performing Organization Name and Address Institute for Computer Applications in Science and Engineering Mail Stop 132C, NASA Langley Research Center Hampton, VA 23665-5225		10. Work Unit No. 11. Contract or Grant No. NAS1-18107
12. Sponsoring Agency Name and Address National Aeronautics and Space Administration Washington, D.C. 20546		13. Type of Report and Period Covered Contractor Report 14. Sponsoring Agency Code 505-90-21-01

15. Supplementary Notes

Langley Technical Monitor: J. C. South

Submitted to AIAA J.

Final Report

16. Abstract

The cell-vertex schemes due to Ni and Jameson, et al. have been subjected to a theoretical analysis of their truncation error. The analysis confirms the authors' claims for second-order accuracy on smooth grids, but shows that the same accuracy cannot be obtained on arbitrary grids. It is shown that the schemes have a unique generalization to axisymmetric flow that preserves the second-order accuracy.

17. Key Words (Suggested by Authors(s))	18. Distribution Statement
numerical approximation, compressible flow, error estimates	02 - Aerodynamics 64 - Numerical Analysis Unclassified - unlimited

19. Security Classif.(of this report)	20. Security Classif.(of this page)	21. No. of Pages	22. Price
Unclassified	Unclassified	42	A03

For sale by the National Technical Information Service, Springfield, Virginia 22161

NASA-Langley, 1987